Kashf Journal of Multidisciplinary Research
Vol: 02 - Issue 12 (2025)
P-ISSN: 3007-1992 E-ISSN: 3007-200X
https://kjmr.com.pk

COMPUTATIONAL ANALYSIS OF TURBULENT FLOW PHENOMENA IN BAFFLED RECTANGULAR CHANNELS: SINGLE VS. DOUBLE STEP CONFIGURATIONS

*[1]Akhalque Ahmed Abbasi, [2]Murtaza Hussain Shar, [3]Mazhar Ali Sahito, [4]Dr. Abdul Raheem Shar**

[1,3]*GRA Govt. Degree College Kandiaro*

[2, 4]*Govt. Degree College Thari Mirwah*

**Corresponding Author:* araheem.shar@salu.edu.pk

Article Info

Abstract

The present work shows computational analysis of fluid flow through a rectangular channel modified by single as well as double baffle steps utilizing the finite element method (FEM) within the COMSOL Multi-physics background. The study focuses on the complex relationship of boundary layer separation, vortex generation, and flow phenomena governed by the incompressible Navier-Stokes and continuity equations. To achieve a numerical solution, these second-order governing equations were converted into a first-order system by introducing vorticity as an additional unknown. Discretization was performed using the Galerkin finite element method coupled with a least squares residual approach to manage non-linearity and higher-order terms, while the Newton-Raphson method was utilized for final calculations. Steady-state simulations conducted across a Reynolds number (Re) range of 1 to 500 reveal that vortex formation is strongly dependent on fluid inertia. Results indicate that while no vortices appear at Re = 1, distinct primary and secondary vortices begin to form in the corners of the step baffles by Re = 50. As Re increases to 200, these vortices merge, and by Re = 500, the consolidated secondary vortex expands significantly to fill the entire channel domain. Comparative analysis between single and double baffle configurations shows that increasing the number of baffles facilitates more energetic and sustained vortex growth, with the double-step geometry reaching a maximum vortex length of approximately 0.20 compared to 0.06 in the single-step design at Re = 500. The numerical results demonstrate strong agreement with established literature, confirming the accuracy of the proposed computational approach for investigating flow efficiency and energy dissipation in baffled channels.

Keywords:

Baffle steps, Rectangular channel flow, Finite element method (FEM), Vortex formation, Reynolds number, Fluid dynamics

INTRODUCTION

Boundary layer separation, vortex formation, and pressure fluctuations interact intricately when studying fluid flow through a rectangular channel altered by single and double baffle steps [1-3]. From a mathematical perspective, the incompressible Navier-Stokes equations, which represent the conservation of mass and momentum, are primarily responsible for this phenomenon [4-6]. The continuity equation$\nabla \cdot u = 0$, guarantees that the mass flux remains stable within the channel, whereas the momentum equation, $\rho(\partial t/\partial u + u \cdot \nabla u) = -\nabla p + \mu \nabla 2u + f$, states the motion of the fluid under the power of pressure gradients and viscous forces [7-9]. When a baffle is introduced, it acts as a rigid geometric constraint where the no-slip boundary condition, **u**=0, is applied at the solid-fluid interface. This interruption of the flow field forces the fluid to accelerate through the narrowed passage, significantly altering the local Reynolds number, $= \rho UL/\mu$, and triggering the formation of recirculation zones or eddies immediately downstream of the baffle step [10,11]. The flow in a single baffle configuration has a single primary wake region and a localized pressure drop. The convective term $u \cdot \nabla u$, which becomes dominant as the fluid is pushed around the baffle's sharp edge, mathematically captures the change from a laminar profile to a disturbed state [12,13]. By creating a "staggered" or "aligned" interaction effect, the addition of a second baffle step raises the complexity. The unsteady wake produced by the first baffle interacts with the second baffle, frequently resulting in increased mixing and sporadic vortex shedding [14]. If the flow is turbulent, this interaction can be modelled using the Reynolds-averaged Navier-Stokes (RANS) approach, where the velocity is broken down into mean and fluctuating components. In order to account for the turbulent momentum and its dissipation rate, additional closure models such as the k-ω or k-ω models are needed [15–17].

These partial differential equations that run over the uneven domain formed by the baffles can be solved mathematically using the Finite Element Method (FEM) [18]. The channel is discretised into a mesh of finite elements, which are typically tetrahedral in three dimensions or triangles or quadrilaterals in two dimensions. The unknown velocity and pressure fields within each element are estimated using shape functions like, $uh = \sum ui\phi i,$ and $ph = \sum pi\psi i$. The continuous governing equations are then converted into a system of algebraic equations using the Galerkin weighted residual approach [19]. FEM solvers frequently use methods like the Penalty Method or the Mixed Finite Element formulation (satisfying the LBB or Inf-Sup condition) to guarantee numerical stability because the Navier-Stokes equations are non-linear and the pressure-velocity coupling is limited by the Incompressibility condition [20]. The outcome is a high-fidelity mapping of the pressure distributions and velocity vectors that makes it possible to quantify the "baffle effect" on the system's overall flow performance and energy loss [21,22].

METHODOLOGY

Galerkin Approximations of the Governing Equations

The Navier-Stokes equations were the main topic of this discussion of the mathematical theory of the governing equations. The various domains of engineering, industry and science all heavily rely on these equations. The differential version of the conservation laws for either mass or momentum can be used to express these equations, which are typically derived from Newton's second law of motion. The local

and material derivatives of a body's acceleration are the main focus of the momentum equation. Because the convection term is involved, these equations are referred to in mathematics as non-linear and higher order partial differential equations. The steady state and transient solutions of several parameters, such as velocity vector field, pressure, and vorticity, are nearly impossible to discover analytically due to higher order and particularly non-linearity conditions. As an alternative, the steady state position of the governing equations requires a numerical solution. However, the numerical solution relies on a large number of iterations in each parameter; hence, a computational setup for a fast and convergent solution is required to regulate the large number of iterations. As a result, the CFD program COMSOL MultiPhysics was selected for the selected physical problem, adopted a numerical solution based on a specific selection of anticipated tools, and may be used in the field of fluid dynamics.

The Governing Equations' Mathematical Theory

The governing equations' mathematical theory is restricted to Newtonian and incompressible fluids, and it is presented in two dimensions using Cartesian coordinates. Here, two equations are discussed: the momentum equation, which is used to move the fluids through the channel, and the continuity equation, which is used to analyse the continuity in fluid flow phenomena.

Continuity Equation

This formula is used to analyse the fluid's continuity as it passes through the channel, concentrating primarily on incompressible fluids with nearly constant densities. Consequently, the continuity equation has the following definition:

$$\frac{\partial u}{\partial x} + \frac{\partial v}{\partial y} = 0 \qquad \textbf{(1)}$$

Momentum Equation

The conservation law of momentum in Cartesian coordinates in both dimension and non-dimension form is a well-known formula that is mostly used in fluid dynamics. It comes from Newton's second law of motion.

Dimension Form

The fundamental equations (1) and (2) are well-known in the field of fluid dynamics; however, in this instance, the fundamental formulas for laminar flow of liquid flows are needed, and they only apply to Newtonian liquids that are transported down the rectangular channel imposing two-step baffles at various bottom wall positions. These equations are written as follows:

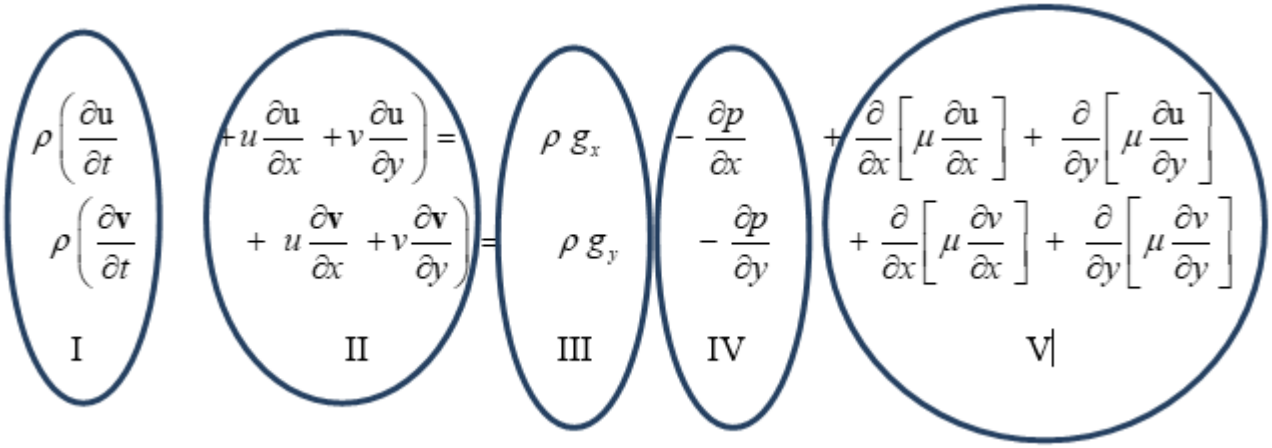

Whereas ρ displays the fluid's density, which stays constant due to the Newtonian fluid, □ displays the fluid's viscosity, which stays constant due to the liquid flowing. Here, I discussed the fluid velocity's time derivative, II its convection, III its exterior forces, IV its pressure, and V its diffusion.

Non–Dimension Form

$$\frac{\partial u}{\partial t}+\left(u\frac{\partial u}{\partial x}+v\frac{\partial u}{\partial y}\right)=-\frac{\partial P}{\partial x}+\frac{1}{Re}\left(\frac{\partial^2 u}{\partial x^2}+\frac{\partial^2 u}{\partial y^2}\right) \tag{3a}$$

$$\frac{\partial v}{\partial t}+\left(u\frac{\partial v}{\partial x}+v\frac{\partial v}{\partial y}\right)=-\frac{\partial P}{\partial y}+\frac{1}{Re}\left(\frac{\partial^2 v}{\partial x^2}+\frac{\partial^2 v}{\partial y^2}\right) \tag{3b}$$

Re, on the other hand, is used to convert a dimension into a non-dimensional form known as the Reynolds number.

Related boundary Conditions

Given the specific and anticipated solution, it is imperative to give the initial and boundary conditions after discussing the mathematical theory of the governing equations. No-slip boundary criteria were used for the channel's solid walls and different baffles, while there was no motion activity within the boundaries. The parabolic classification of the governing equations, which are defined below, fixes the parabolic velocity profile at the inlet. Additionally, zero pressure was applied at the channel's outlet.

$$u(y)=6\times U_m\times\frac{y}{L}\left(1-\frac{y}{L}\right),\ \mathrm{P}=\mathrm{P}_{\max} \tag{04}$$

L is defined as the channel's overall length.

COMSOL MULTIPHYSICS and the Cfd Tool used to select the numerical methodology

Here, the most recent CFD tool, COMSOL Multi-Physics, is used to adopt the numerical methodology. Here, the Galerkin approach is used in conjunction with the finite element method as the numerical tool. Since the governing equations for the velocity field, pressure, and vorticity data are based on higher order and nonlinearity, the least squares approach was used for easy management. The Galerkin calculus with least squares approach is used to discretise the governing equations into independent variables in the form of an arrangement of first-order differential equations. The Newton Raphson method was then used to determine the velocity, pressure, and vortex at the smallest cutoff level 10-5. The COMSOL Multi-Physics application focuses solely on the finite element approach, which is widely used in engineering and the sciences.

Finite Element Method

The finite element approach is a portion of the numerical forecasting used to compute boundary value problems centered on partial differential equations that led to an ensemble of discrete variable equations and identified the closest possible solution of all unknowns under the domain.

Richard Courant first used Fem in 1940 to address a variety of structural mechanics issues, and it was later expanded to include solid and fluid mechanics. By using FEM, a vast domain was split up into several little parts known as finite elements, and each element's single piece solution was then aggregated. By lowering the related mistakes, FEM used the calculus of the differences for the anticipated solution. The FEM concentrated on several dimensions, such as 1D, 2D, and 3D, for a variety of scientific, technical, and large-scale industrial problems involving partial differential equations. These tools can be readily used on an individual basis for linear, quadratic, and quadrilateral operations, such as

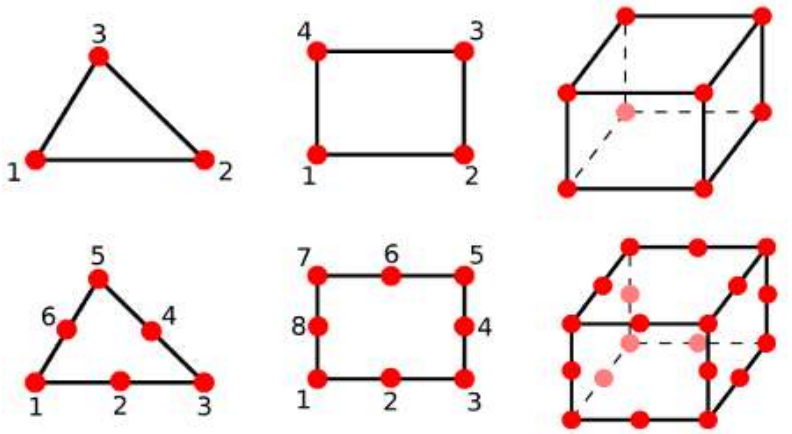

Triangle element with 3 and 6 nodes | Rectangle element with 4 and 8 nodes | Box element (for 3D) with 8 and 20 nodes

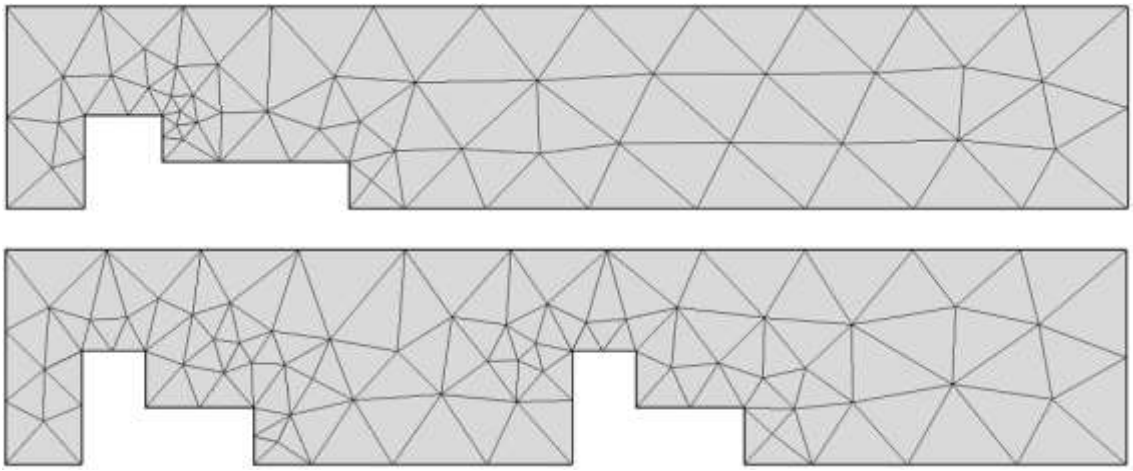

Figure – 2: Various forms of the infinite components

Since 1940, the limited component instrument has been used to solve large variotional problems using computational programming code. These days, the most advanced COMSOL Multi-Physics, ANSYS, and Flex-PDE computational products automatically apply different FEM schemes, and computational packages begin by combining the FEM technique to govern the computations of the various parameters. The Galerkin and Petrov–Galerkin discretisation processes, among other FEM tools, are included in the COMSOL Multi-Physics package. Additionally, the FEM tool is used in conjunction with other numerical methods such as Taylor and least squares procedures. In order to estimate the steady state solution of the velocity field in two dimensions, the Galerkin approach with the choice of least squares procedure was used in this investigation of the various FEM tools.

Step-by-Step Lsgfem Application Process for First Order Systems

Initially, the governing equations are 2nd order partial differential equations, like momentum transfer equations; however, in this instance, the least squares approach utilising FEM is chosen. Since this method is limited to first order systems or equations that govern with one or more parameters, the second order term was reduced to the first order system through adding further unknowns, such as vorticity. The system produced a first order method of equations with the velocity field, vortices, and pressure unknowns by the adoption of vortices in the second order term (diffusion term). The process is implemented as follows:

$$\nabla . \boldsymbol{u} = 0 \tag{5}$$

$$\nabla P + \boldsymbol{u}(\nabla \boldsymbol{u}) = \frac{1}{\mathrm{Re}} \nabla^2 \boldsymbol{u} \tag{6}$$

Here, the additional unknowns are referred to as vorticity and are explained as follows:

$$\boldsymbol{w} = \nabla \times \boldsymbol{u} \tag{7}$$

Utilizing the vector identity in the manner described below;

$$\nabla \times (\nabla \times u) = -\nabla^2 .u \tag{8}$$

When identities (7) and (8) were substituted into the system (6), the system looked like this:

$$\nabla . \boldsymbol{u} = 0 \tag{9a}$$

$$\boldsymbol{u}.\nabla \boldsymbol{u} + \frac{1}{\mathrm{Re}} \nabla \times \boldsymbol{w} + \nabla p = 0 \tag{9b}$$

$$w - \nabla \times \boldsymbol{u} = 0 \tag{9c}$$

As demonstrated here, the two-dimensional research conundrum of a channel with baffles is limited to Newtonian and incompressible fluids;

$$\frac{\partial \mathrm{u}}{\partial x} + \frac{\partial \mathrm{v}}{\partial y} = 0 \tag{10a}$$

$$u \frac{\partial u}{\partial x} + v \frac{\partial u}{\partial y} + \frac{\partial P}{\partial x} + \frac{1}{\mathrm{Re}} \frac{\partial w}{\partial y} = 0 \tag{10b}$$

$$u \frac{\partial \mathrm{v}}{\partial x} + v \frac{\partial \mathrm{v}}{\partial y} + \frac{\partial P}{\partial y} - \frac{1}{\mathrm{Re}} \frac{\partial \mathrm{v}}{\partial x} = 0 \tag{10c}$$

$$w + \frac{\partial u}{\partial y} - \frac{\partial v}{\partial x} = 0 \tag{10d}$$

The above system (10) is a first order system with vorticity (w), pressure unknowns (P), and velocity field (u and v). The FEM technique allows it to be converted into a matrix representation of velocities field with respect to parameters like x and y.

$$\mathrm{A}_1 = \begin{pmatrix} 1 & 0 & 0 & 0 \\ u & 0 & 1 & 0 \\ 0 & u & 0 & -\frac{1}{\mathrm{Re}} \\ 0 & -1 & 0 & 0 \end{pmatrix}, \qquad \mathrm{A}_2 = \begin{pmatrix} 0 & 1 & 0 & 0 \\ v & 0 & 0 & \frac{1}{\mathrm{Re}} \\ 0 & v & 1 & 0 \\ 1 & 0 & 0 & 0 \end{pmatrix}$$

$$\mathrm{A} = \begin{pmatrix} 0 & 0 & 0 & 0 \\ 0 & 0 & 0 & 0 \\ 0 & 0 & 0 & 0 \\ 0 & 0 & 0 & 1 \end{pmatrix}, \qquad f = \begin{pmatrix} 0 \\ 0 \\ 0 \\ 0 \end{pmatrix}, \qquad \mathbf{u} = \begin{pmatrix} u \\ v \\ p \\ w \end{pmatrix}$$

The aforementioned matrices' matrix form is expressed as KU = F, where K is referred to as the stiffness matrix that gathered from the least squares process as shown below;

$$L\Psi_j = \Psi_{j,x} A_1 + \Psi_{j,y} A_2 + \psi_j \Psi \tag{11a}$$

$$K_e = \int_{\Pi_d} <L\Psi_1, L\Psi_2, L\Psi_3, ..., L\Psi_{Ne}>^T < L\Psi_1, L\Psi_2, L\Psi_3, ..., L\Psi_{Ne}> d\Pi \tag{11b}$$

The differential system is discretised into the different discrete unknowns from (11), leading to an algebraic system of equations for all unknowns, including vorticity, pressure, and velocity field. To complete the calculations of all unknowns, a specific numerical tool is now required. The Newton's method, also called the Newton Raphson method, is an iterative process that is defaulted in the COMSOL Multi Physics module.

Newton Raphson Method

Two academics named Burden and Faires invented this technique in 2005, and at the time, it was limited to solving single linear and nonlinear equations with a single unknown. However, as computer technology was developed, computational packages were introduced. The following describes the general structure of Newton's technique for a single unknown:

$$z^*_{i+1} = z^*_i - \frac{f(z^*_i)}{f'(z^*_i)} \qquad i = 0, 1, 2, 3, ... \tag{12}$$

For several unknown computations, the equation (3–12) can be moved into the subsequent process.

$$z^*_{i+1} = z^*_i - J(z^*_i)^{-1} f(z^*_i) \qquad i = 0, 1, 2, 3, ... \tag{13}$$

is defined here as an inverse matrix made up of all derivatives of unknowns with respect to x and y; additionally, it is defined as a Jacobean matrix, which is created as follows:

$$J(x)^{-1} = \begin{bmatrix} \frac{\partial f_1}{\partial x_1}(x) & \frac{\partial f_1}{\partial x_2}(x) ..... & \frac{\partial f_1}{\partial x_n}(x) \\ \frac{\partial f_2}{\partial x_1}(x) & \frac{\partial f_2}{\partial x_2}(x) ..... & \frac{\partial f_2}{\partial x_n}(x) \\ . & . ..... & . \\ . & . ..... & . \\ . & . ..... & . \\ \frac{\partial f_n}{\partial x_1}(x) & \frac{\partial f_n}{\partial x_2}(x) ..... & \frac{\partial f_n}{\partial x_n}(x) \end{bmatrix}$$

For the (13) system, the initial guesses for each unknown must be described separately, and the converging solution must then be calculated by numerous iterations.

RESULTS AND DISCUSSION

The flow through rectangular channels with different kinds of baffles is closely related to hydraulic engineering and is extensively utilized in the field of hydrodynamics, especially for flow calculations and the development of the mechanism of water surface level in open channels. It controls the pressure distributions in the hydrostatic field and is also available in crest wiring. The study of baffles is not restricted to a specific subject; rather, it is unmitigated in the field of heat transmit to investigate heat capacity via baffle plates in the electrical devices with closed bodies. Additionally, the biosciences use the baffles thought to evaluate blood flow via veins and arteries in the incidence of various disorders such stenosis and fat availability in the arteries. In order to investigate broad crested weirs through open channels, [23] created a projected model with the goal of examining the water level and controlling the pressure distribution upstream. The CFD (computational fluid dynamics) program Fluent was utilised for the turbulent modelling of crested weirs utilising the k−ε turbulent model, in addition to evaluating the water level in large machinery laboratory to measure experimental measures.

Gambit, another CFD application, was also utilised to create both unstructured as well as structured meshes with single and double steps in the open channel. The various factors at the entry of the open channel, including energy dissipation, the water surface profile, and the air and liquid flows, were calculated both experimentally (limited) and numerically (mostly). The forecasts of broad crested weirs and energy dissipation outcomes were shown to be superior to the heavy equipment experimental investigations.

The same issue was expanded by [23] using a variety of experimental studies and a CFD program. Fluent with Gambit forecasts of the wide crested weirs across the open channel with solid baffle steps fixed at different bottom wall locations. Additionally, they noticed that the step baffle's height and length changed in the open channel flows. The water level surface profile was calculated using a variety of numerical tools, including the k-ε model, k-ω model, RNG k-ε model, and realizable k-ε model. The relative inaccuracy of each approach was then calculated using experimental investigations. The results showed that the k–ε model, with its lowest relative error of 5.11%, was superior to all numerical tools for studying turbulent flow processes.

Definition a Problem with Conditions

Only Newtonian fluid behavior is investigated here. The predicted least square finite element method is used to solve the continuity and momentum equation. Baffle steps, both single and double, are fastened to the channel's lower wall. The channel's stationary walls and the walls of the baffles are subject to no-slip boundary conditions, which are fixed in the channel's schematic diagram. There is a fixed zero pressure at the channel's outflow and an imposed parabolic velocity profile at the entrance. On the entire domain, the triangular element with the smallest element size is selected for the finite element discretisation. The following table describes the mesh's detailed structure for both problems. The CFD

program COMSOL Multi-Physics is used to calculate the expected findings, and the velocity field flow patterns are verified using the other flow patterns of [23].

Table: 1 Comparison of Mesh Statistics and Element Quality for Single vs. Double Stirrer Configurations

Description	Single Stirrer Value	Double Stirrer Value
Vertex elements	10	16
Edge elements	254	284
Triangular elements	4386	4602
Average element quality	0.988	0.9882
Minimum element quality	0.7491	0.8514

Finite Element

The CFD program COMSOL MultiPhysics is used to fully compute the expected outcomes using the Galerkin FEM method addition with least square residuals. The following consequences of the fluid flow phenomenon serve as the foundation for the post-process results:

Modification of Fluid Inertia on Flow Characteristics via Rectangular Channel with Baffles

A parabolic velocity profile at the intake, zero pressure applied to the channel's exit, and no-slip boundary conditions on stationary walls are only a few of the zones that are defined in the schematic diagram shown in figure 1. Figure 2 shows the finer, very fine meshes of the rectangular channel with fixed two-step baffles at the single and double baffles at the lower wall. Figures 3(a) and 3(b) show the streamline patterns of the velocity field at different lower and higher Reynolds numbers from 01 to 500 via the rectangular channel made by the two-step baffle at a single location on the bottom wall. Small vortices first developed in each corner of the step baffles at Re = 01. The left corner vortex vanished as Re climbed, and the primary and secondary vortices gradually grew horizontally as Re went up to Re -100. Additionally, these are the same streamline flow patterns for high Reynolds numbers (200, 300, and 500). The left corner vortex essentially disappears in huge Re's. However, the primary vortex gradually intensifies and merges with the secondary vortex from Re-200. As a result, the secondary vortex fills the entire channel and increases significantly with increasing Re's up to Re = 500.

The velocity field's streamline patterns through channel-imposed two-step baffles at the bottom wall's double positions are displayed in Figure 4.4. In a similar vein, little eddies were seen at each step in both single and double places on the bottom wall. Eddies become larger at every stage in every location up to less than 200 Rs as a result of a rise in the Reynolds number. The initial primary and secondary vortices combined at Re = 200, but the second primary and secondary vortices grew larger and shifted in the direction of the domain's outflow.

Furthermore, at every channel step, Re = 300 main eddies (first and second) combine to form secondary eddies. The eddies get bigger as the Reynolds number increases, and the second secondary eddies keep

getting bigger until they fill the entire domain at the Reynolds number (= 500). The vortices are plainly visible at every corner of the channel as a result of increasing Re's. In the first step, the primary and secondary vortices combine at Re=500, and in the second step, the vortices grow and take up space in the step and channel at Re=500.

Impact of Increasing the Rectangular Channel's Baffle Count

The streamline patterns of flow and vortex phenomenon through the channel are affected by the presence of two-step baffles. Figure 5(a) shows how the baffles affect the fixed Reynolds numbers (01 and 150). The vortices are not visible in the channel's baffle steps in both single and double wall locations because to the low Reynolds number (01). Additionally, Vortices with a Reynolds number of roughly 150 were seen in the various stages of the baffles at single and double positions of the wall. Both the single and double sites of the wall have eddies that are nearly identical in size. Additionally, both secondary and primary vortex start to combine in specific areas of the wall as the value of Reynolds (200) is raised in figure 5(b). However, when two step baffles are increased, the first primary and secondary vortices fully merge, and the second primary and secondary vortices are observed at the second location of the wall. As a result of the increased number of two-step baffles, with higher Reynolds numbers (=500), all primary eddies at first and second locations entirely mix with secondary eddies at every position of the wall and occupy the entire domain.

Figure 6, which is based on plots of the recirculation flow rate caused by an increase in Reynolds number, confirms the continual improvement seen in the two-step baffles with a rising Reynolds number. The enhancement is displayed in Figure 6(a) up to the limited Reynolds number of 200. Additionally, the combined primary and secondary vortices prevented the enhancement from being seen in the plots. However, as the Reynolds number increases, the recirculation flow rate is shown to be continuously growing in figure 6(b). In a similar vein, another flow characteristic is calculated as the secondary vortex length on the Reynolds number shift. Additionally, it noted that the vortex size gradually increased as the Reynolds number increased. Empirical equations that focus on the maximum value of the recirculation flow rate on various Reynolds numbers are another phenomenon that has emerged as a novel contribution. The individual descriptions of the empirical equations are as follows:

Baffles with two steps in one place

$$Xs = 2.72e-06\,\mathrm{Re} + 1.0e-04 \qquad 1 \le \mathrm{Re} \le 500$$

Baffles with two steps at two different places

$$X_D = 1.4821e-06\ \mathrm{Re} + 2.23786e-06 \qquad 1 \le \mathrm{Re} \le 500$$

Table 2: Comparison of Minimum and Maximum Recirculation Flow Rates (□) at Varying Reynolds Numbers (Re) for Single and Double Stirrers

Recirculation Flow Rate (□)					
Reynolds Number (Re)	Single Stirrer		Reynolds Number (Re)	Double Stirrer	
	(□1 min)	(□1 max)		(□1 min)	(□1 max)
500	6.73×10^{-9}	1.36×10^{-3}	500	2.98×10^{-8}	7.39×10^{-4}
400	1.20×10^{-9}	1.09×10^{-3}	400	2.38×10^{-8}	5.95×10^{-4}
300	8.76×10^{-10}	8.04×10^{-4}	300	1.81×10^{-9}	4.53×10^{-4}
200	6.75×10^{-10}	5.17×10^{-4}	200	4.04×10^{-9}	3.03×10^{-4}
100	2.22×10^{-10}	2.74×10^{-4}	100	1.52×10^{-9}	1.49×10^{-4}
1	4.06×10^{-11}	2.83×10^{-6}	1	2.64×10^{-12}	1.47×10^{-6}

The CFD tool COMSOL Multi-Physics is used to calculate the expected findings for the study of the Newtonian fluid transported via the rectangular channel enforced two step baffles at single and double locations of the lower wall. Galerkin finite element analysis with coupling the least squares method is used to construct the velocity vector field using the momentum equation and continuity equations for incompressible fluids. The different Reynolds numbers were the main focus of the flow phenomenon. Various flow characteristics, such as vortex length, recirculation flow rate, and streamline flow features, are noted. The vortex phenomenon was examined at the corners of each step fitting in the channel. At lower Reynolds numbers, a very little vortex was seen, and as the Reynolds number climbed, the vortex's size gradually increased. The single and double stirrers' minimum and maximum values of the vortex length (X) and recirculation flow rate at various Reynolds numbers.

Table: 3 Reynolds numbers (Re) on the stationary single and double stirrer determine the vortex length (X)

Vortex Length (X)			
Reynolds Number (Re)	Single Stirrer(XS)	Reynolds Number (Re)	Double stirrer (XD)
500	0.06	500	0.20
400	0.06	400	0.17
300	0.06	300	0.11
200	0.04	200	0.034
100	0.02	100	0.02
01	0.01	01	0.01

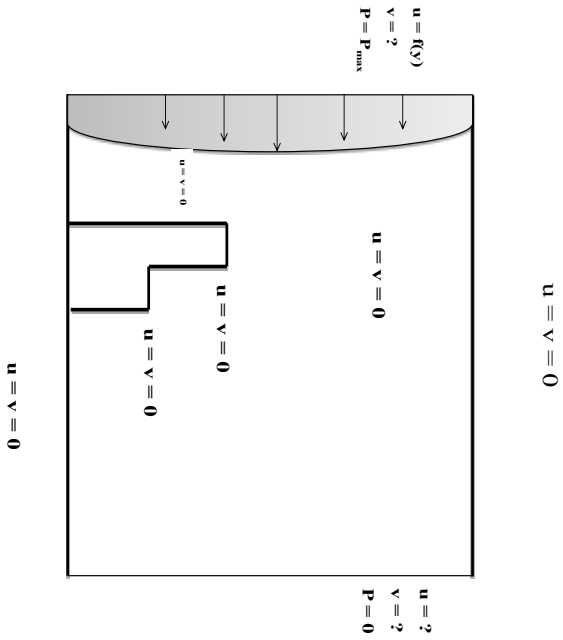

Figure: 1 Schematic drawing illustrating the two-dimensional rectangular channels along the lower wall with fixed two-step barriers at various locations.

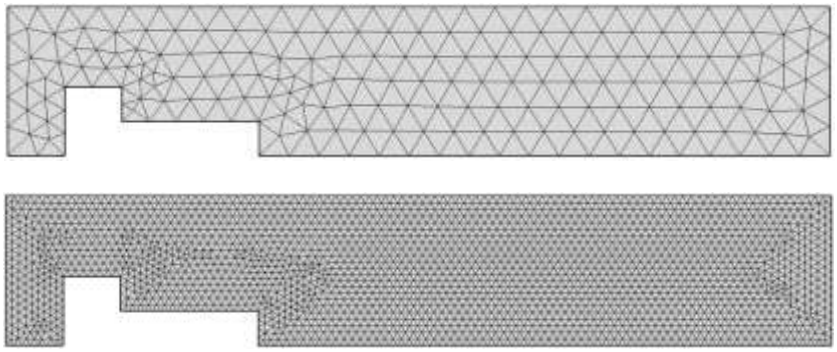

(a)

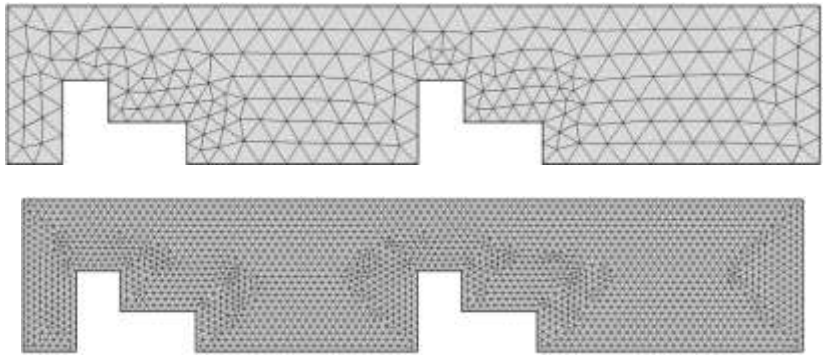

(b)

Figure: 2(a & b): The rectangular channel's mesh is incredibly fine, with fixed 2-step baffles at different points along the wall

Re=01

Re=50

Re=100

Re=150

Figure – 3(a): Visualizing Velocity Patterns and Streamlines around a Fixed Two-Step Obstacle in Low-Reynolds Number Flow (01 ≤ Re ≤ 150).

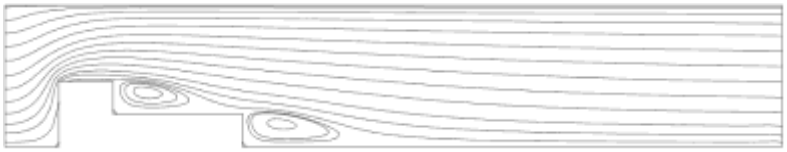

Re=200

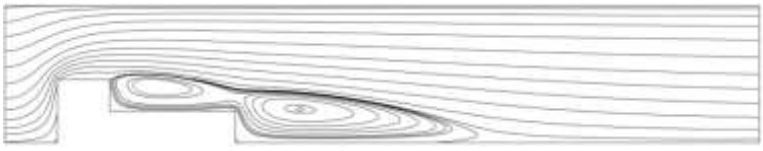

Re=300

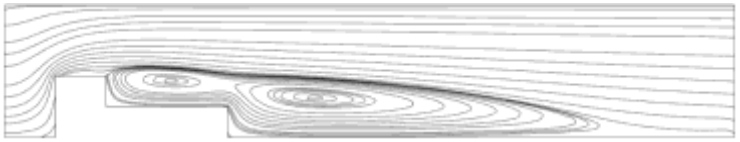

Re=400

Re=500

Figure – 3(b): Steady-State Laminar Flow Field and Streamline Analysis of a Two-Step Baffle within a Rectangular Duct (200 ≤ Re ≤ 500).

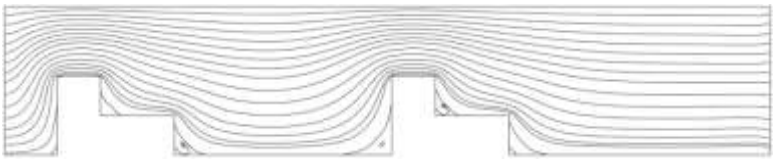

Re=01

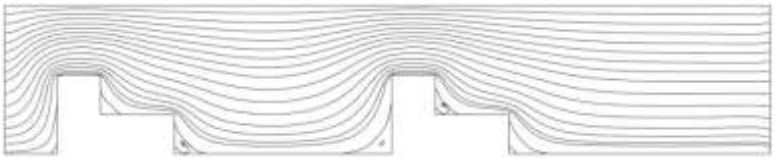

Re=50

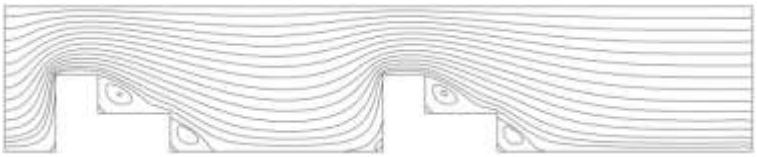

Re=100

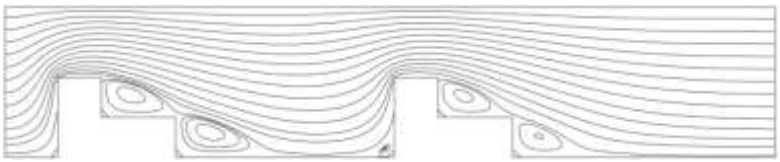

Re=150

Figure – 4(a): Characterizing Flow Interaction and Velocity Patterns between Tandem Two-Step Baffles at Low Reynolds Numbers (01 ≤ Re ≤ 150).

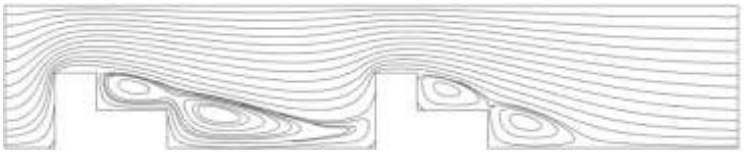

Re=200

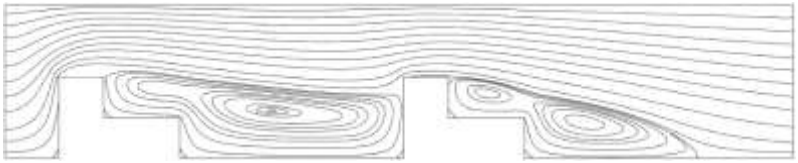

Re=300

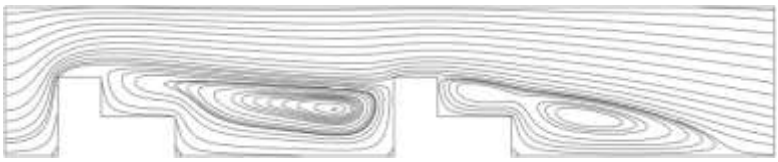

Re = 400

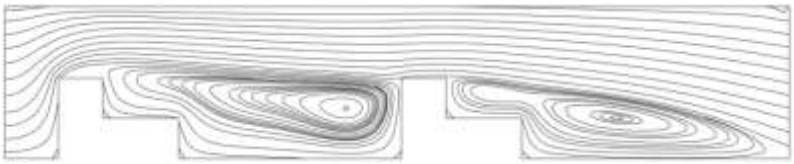

Re=500

Figure – 4(b): Velocity Field Patterns and Recirculation Zones for Multiple Step-Baffles at Moderate Reynolds Numbers (200 ≤ Re ≤ 500).

Re=01

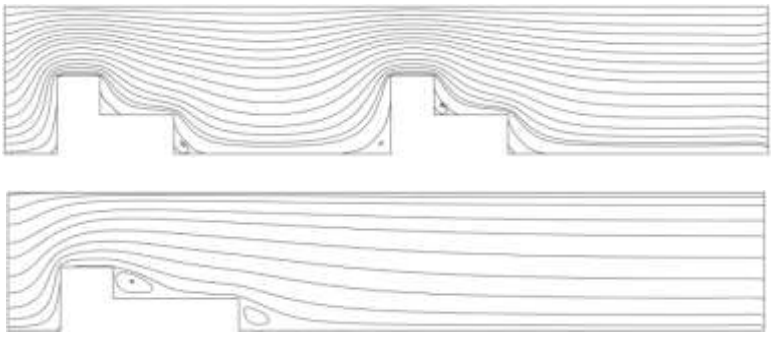

Re=150

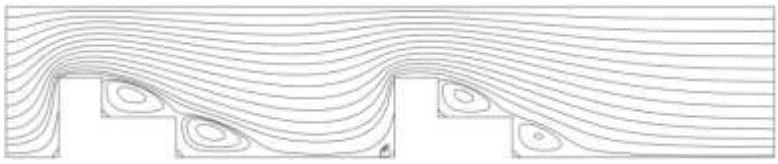

Figure –5(a): Transition from Creeping Flow to Vortex Formation: A Study of Single and Double Two-Step Baffles (Re = 01 and Re = 150).

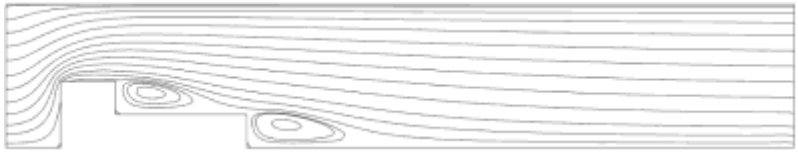

Re=200

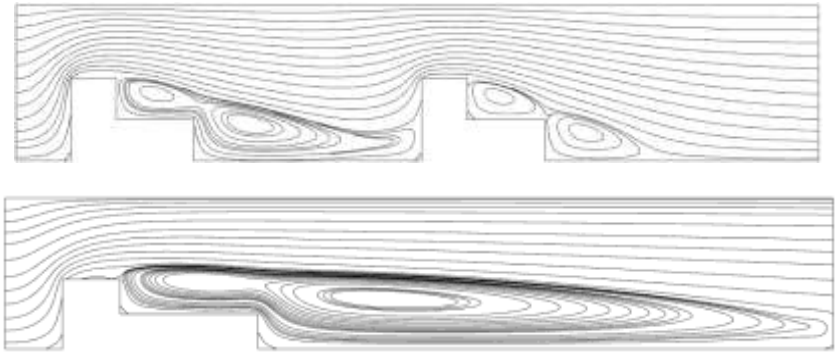

Re=500

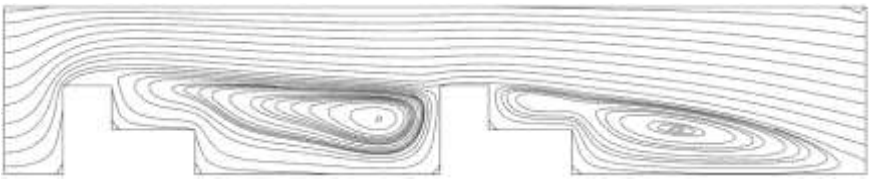

Figure –5(b): Evolution of Wake Interactions and Recirculation Zones for Single and Tandem Two-Step Baffles (Re = 200 and Re = 500).

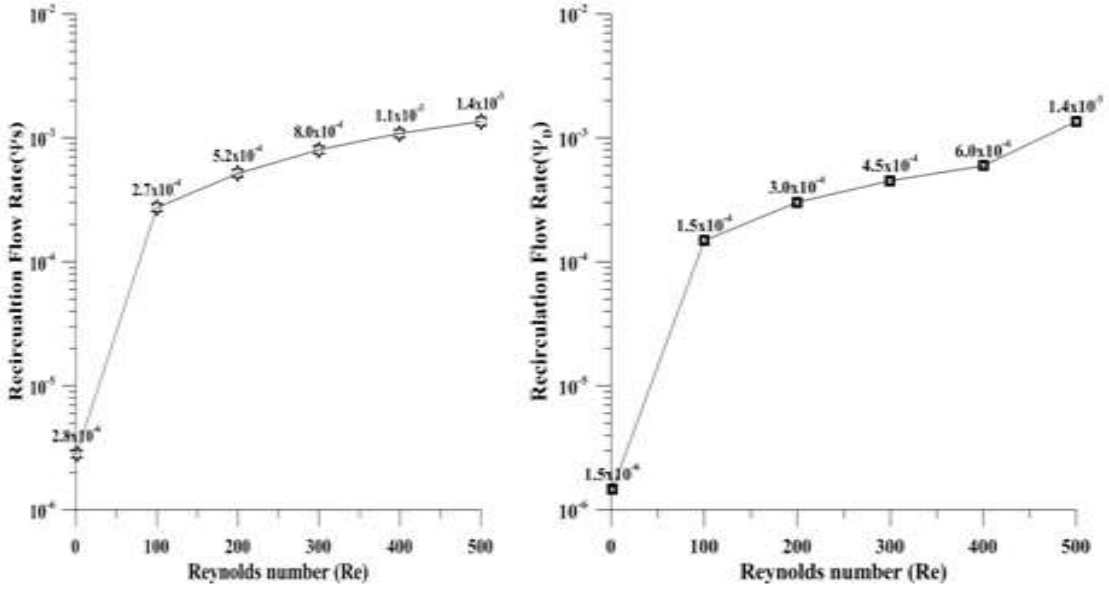

Figure –6: Variation of Recirculation Flow Rate (Y) Across Multiple Reynolds Numbers and Baffle Configurations

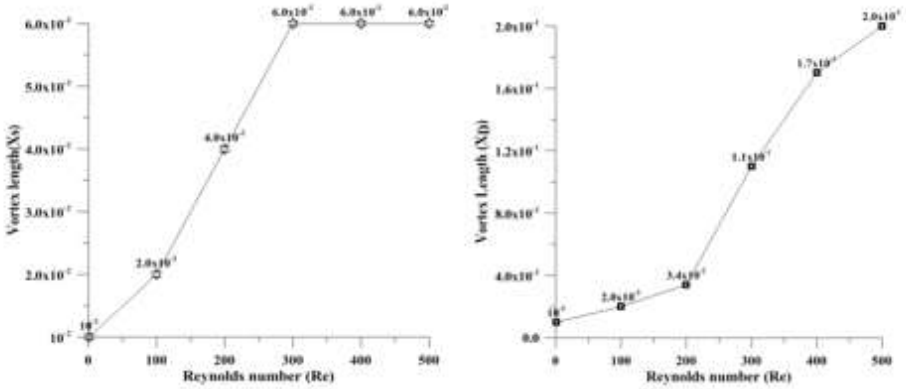

Figure –7: Relationship between Reynolds Number and Downstream Vortex Extension (X) in Baffled Rectangular Channels

Conclusion

The Reynolds number (Re) has a significant impact on vortex dynamics, as shown by the computational study of fluid flow through a rectangular channel with single and double baffle steps. There are no vortices at a low Reynolds number of 1, but as Re rises to 50, distinct primary and secondary vortices start to form at each baffle step's corners. With additional increases in Re, these vortices progressively increase in size and intensity before merging to form consolidated flow structures around Re = 200. The secondary vortices greatly enlarge by Re = 500, with the double-step configuration's downstream secondary vortex taking up the majority of the channel domain. These flow characteristics are further improved by adding more baffles. The double baffle configuration maintains continuous growth, reaching a maximum length of 0.20 at Re = 500, whereas the vortex length in a single baffle configuration plateaus at roughly 0.06 for Re ≥300. Similarly, compared to the single baffle configuration, where growth slows down following vortex merging, the recirculation flow rate increases more dramatically and steadily in the double baffle geometry. Double baffle configurations are more efficient at producing energetic and sustained re-circulating structures, which are crucial for applications requiring improved mixing or energy dissipation, according to these findings, which are supported by strong agreement with the body of existing literature.

Author Contribution

Akhalque Ahmed Abbasi conceptualized and designed experiments, Dr. Abdul Raheem Shar prepared the draft of the article Murtaza Hussain Shar interpreted the data Mazhar Ali Sahito, performed statistical analysis, All authors read, revised, and approved the final version of the manuscript.

Acknowledgements

The authors acknowledge the facilities provided by the Institute of Mathematics, Shah Abdul Latif University Khairpur and also technical support provided by department of Statistics Shah Abdul Latif University Khairpur.

Conflict of Interest

The authors declare no conflict of interest.

References

1. Li, J.H., Wang, B.F., Qiu, X., Zhou, Q., Fu, S.X. and Liu, Y.L., 2024. Vortex dynamics and boundary layer transition in flow around a rectangular cylinder with different aspect ratios at medium Reynolds number. Journal of Fluid Mechanics, 982, p.A5.

2. Saha, S., Biswas, P., Nath, S. and Singh, L., 2021. Numerical simulations of Newtonian fluid flow through a suddenly contracted rectangular channel with two different types of baffle plates. Soft Computing, 25(15), pp.9873-9885.

3. Zhan, Y., Zhang, H. and Zhang, S., 2025. Numerical investigation of flow and heat transfer characteristics in a rectangular channel with perforated inclined baffle. International Communications in Heat and Mass Transfer, 164, p.108941.

4. Temam, R., 2024. Navier–Stokes equations: theory and numerical analysis (Vol. 343). American Mathematical Society.

5. Wang, S., 2022. Extensions to the Navier–Stokes equations. Physics of Fluids, 34(5).

6. Zaza, D., 2021. On modified Navier-Stokes equations for viscous non-Newtonian incompressible fluid motion and their numerical solution (Doctoral dissertation, Politecnico di Torino).

7. Pinelli, M., Herlina, H., Wissink, J.G. and Uhlmann, M., 2022. Direct numerical simulation of turbulent mass transfer at the surface of an open channel flow. Journal of Fluid Mechanics, 933, p.A49.

8. Nandagopal, N.S., 2023. Fluid Mechanics and Momentum Transfer. In Chemical Engineering Principles and Applications (pp. 175-267). Cham: Springer International Publishing.

9. Wei, T., Li, Z. and Wang, Y., 2024. New momentum integral equation applicable to boundary layer flows under arbitrary pressure gradients. Journal of Fluid Mechanics, 984, p.A64.

10. Meng, Y., Romero-García, V., Gabard, G., Groby, J.P., Bricault, C., Goudé, S. and Sheng, P., 2022. Fundamental constraints on broadband passive acoustic treatments in unidimensional scattering problems. Proceedings of the Royal Society A, 478(2265), p.20220287.

11. Saha, S. and Hasan, N., 2024. Numerical evaluation of thermohydraulic parameters for diverse configurations of shell-and-tube heat exchanger. Results in Engineering, 23, p.102509.

12. Betz, M., Gleiss, M. and Nirschl, H., 2021. Effects of Flow baffles on flow profile, pressure drop and classification performance in classifiers. Processes, 9(7), p.1213.

13. Hasan, M.S., 2022. Numerical study of the impact of baffle on flow and heat transfer inside a skewed enclosure.

14. Hirom, K., 2024. Investigating the Impact of Inclined Plates and Perforated Baffles on Sedimentation Tank Performance through Computational Fluid Dynamics Modelling (Doctoral dissertation, NATIONAL INSTITUTE OF TECHNOLOGY).

15. Hami, K., 2021. Turbulence Modeling a Review for Different Used Methods. International Journal of Heat & Technology, 39(1).

16. Niazi, M., Ashrafizadeh, S.N. and Hashemabadi, S.H., 2024. Improving the prediction of turbulent kinetic energy for drag reduction in turbulent viscoelastic pipe flow. Physics of Fluids, 36(6).

17. Kalia, N., 2025. Turbulence Closure Modeling Using Kolmogorov-Arnold Networks and Bayesian Optimization.

18. Gao, H., Yin, Z., Liu, J., Zang, Q. and Lin, G., 2021. Finite element method for analyzing effects of porous baffle on liquid sloshing in the two-dimensional tanks. Engineering Computations, 38(5), pp.2105-2136.

19. Shylaja, G., Venkatesh, B., Naidu, V.K. and Murali, K., 2021. Two-dimensional non-uniform mesh generation for finite element models using MATLAB. Materials Today: Proceedings, 46, pp.3037-3043.

20. Iweobodo, D.C., Njoseh, I.N. and Apanapudor, J.S., 2023. A new wavelet-based galerkin method of weighted residual function for the numerical solution of one-dimensional differential equations. Mathematics and statistics, 11(6), pp.910-916.

21. Heblekar, T.Y. and Reddy, J.N., 2025. An improved dual mesh control domain formulation for the unsteady flow of viscous incompressible fluids. Physics of Fluids, 37(3).

22. Velasco Vega, D.S., 2025. Modeling Steady-State Navier-Stokes Flow Using Structure-Preserving Truncated Hierarchical B-Splines.

23. Dissanayaka, K.D.C.R., Tanaka, N. and Hasan, M.K., 2024. Numerical simulation of flow over a coastal embankment and validation of the nappe flow impinging jet. Modeling Earth Systems and Environment, 10(1), pp.777-798.